# Wildfire-driven $N-k$ contingency generation for security-constrained AC optimal power flow in the California power grid


Irabiel Romero
*Applied Mathematics*
*University of California, Merced*
Merced, CA
iromeroruiz@ucmerced.edu

Nai-Yuan Chiang
*Center for Applied Scientific Computing*
*Lawrence Livermore National Lab*
Livermore, CA
chiang7@llnl.gov

Ignacio Aravena
*Computational Engineering Division*
*Lawrence Livermore National Lab*
Livermore, CA
aravenasolis1@llnl.gov

Roummel Marcia
*Applied Mathematics*
*University of California, Merced*
Merced, CA
rmarcia@ucmerced.edu

Noemi Petra
*Applied Mathematics*
*University of California, Merced*
Merced, CA
npetra@ucmerced.edu

Jean-Paul Watson
*Center for Applied Scientific Computing*
*Lawrence Livermore National Lab*
Livermore, CA
watson61@llnl.gov

Cosmin G. Petra
*Center for Applied Scientific Computing*
*Lawrence Livermore National Lab*
Livermore, CA
petra1@llnl.gov



***Abstract*—The power grid is a critical infrastructure that ensures a continuous supply of electricity to homes, businesses, and essential services, forming the backbone of modern society and economic activities. The increased risk of wildfires is widely recognized to pose significant threats to grid stability, as these events cause spatially correlated, simultaneous outages of transmission lines, transformers, and generators. Unlike traditional $N-1$ or $N-2$ contingencies that assume independent component failures, this work develops a wildfire-aware security-constrained AC optimal power flow (SC-ACOPF) methodology that integrates wildfire perimeter data with transmission network topology to generate realistic $N-k$ contingency scenarios. By defining configurable safe distance parameters around fire perimeters, the approach identifies at-risk infrastructure and formulates an integrated optimization problem that simultaneously minimizes generation costs and contingency response costs. The methodology is validated on four major California wildfires, demonstrating real-time computational performance and economic benefits compared to sequential optimization approaches while maintaining grid reliability across all wildfire contingencies.**



***Index Terms*—Security-constrained AC optimal power flow (SC-ACOPF), wildfire contingencies, spatially correlated outages, $N-k$ contingency planning**


## I. Introduction

Resilient and economic operation of the electrical power system during wildfires is challenging because of the uncertain ways in which the fires spread and impact the power infrastructure. As wildfires are expected to become more widespread and unpredictable, they not only threaten physical grid assets but also complicate power grid operations, such as day-ahead scheduling, reserve procurement, and emergency restoration strategies. Grid operators are also forced to induce outages and large public safety power shutoffs, essentially de-energizing power lines close to high-risk wildfire perimeters. It is generally accepted that wildfires are increasing risk and uncertainty in grid operations, challenging grid operators and utilities to maintain reliable grid operations [8], [16].

Traditional contingency in power systems focuses on common equipment failures and scheduled maintenance outages. However, the increasing frequency and severity of wildfires, particularly in regions like California, necessitate a more comprehensive approach that accounts for spatially correlated, weather-driven events that can simultaneously threaten multiple grid components. Unlike independent equipment failures, wildfires can simultaneously impact transmission lines, generators, and transformers across large geographic areas, creating cascading effects. In this paper, we focus on the mathematical formulation and computational framework for wildfire-aware security-constrained AC optimal power flow problems.

*Related work.* The proposed computational and modeling framework falls under the umbrella of security-constrained AC optimal power flow (SC-ACOPF) [1]. Central to this framework is the Optimal Power Flow (OPF) problem, one of the most fundamental optimization problems in power system operation and planning. Introduced in the 1970s [3], OPF determines the best operating point of a power grid by minimizing a user-defined objective function, e.g., total generation cost, while satisfying governing physical laws, e.g.,

Kirchhoff's laws, along with engineering limits such as generation capacities, line thermal limits, and bus voltage bounds. The Alternating Current OPF (ACOPF) formulation captures the full nonlinear and nonconvex nature of real power systems by explicitly modeling both active and reactive power as well as a wide range of practical operating constraints, making it more accurate but computationally challenging to solve [7]. However, solving the ACOPF for the base case alone—under long-term steady-state operating conditions is not sufficient to guarantee secure system operation when contingencies occur.

The SC-ACOPF extends the ACOPF by incorporating contingency scenarios directly into the optimization: the objective remains to minimize base-case generation costs, but the solution must also guarantee feasibility under all predetermined contingencies. In the context of this work, the security constraints ensure that ACOPF-based grid controls are not only feasible under normal operating conditions but also robust to disturbances that occur when wildfires encroach on power grid infrastructure. Namely, wildfire contingencies model grid components—generators, lines, and transformers—that may be damaged or de-energized due to their proximity to the wildfire perimeter, for example, to reduce the risk of ignition of natural vegetation. These are effectively $N-k$ contingencies, where the number $k$ of unavailable grid elements is generally much larger than one, which is a significant departure from previous work in [14] and poses significant convergence issues for Newton-Raphson solvers for contingency ACOPF [4], [5], [9], [18], [20]. Generally, multiple such wildfire contingencies need to be incorporated in the SC-ACOPF model due to the uncertain wildfire path that arises from weather and local terrain conditions. For each contingency, our SC-ACOPF model redispatches power generators within prescribed ramping limits to ensure that the system remains feasible with respect to power flows and thermal line limits on the new topology, while requiring minimal load shedding.

Wildfire impact on power grid has been investigated previously in various contexts: restoration and public safety power shutoffs [15], [16], mitigation of dynamic instabilities [2], co-optimization of wildfire risk mitigation and load shedding [8], [19]. The multi-period OPF framework proposed recently in [8] is capable of handling large power grids (using linear models) and multiple wildfire contingencies. However, we differentiate from this work by considering the more realistic, nonlinear ACOPF models and focusing on numerical optimization and modeling artifacts that allow obtaining real-time solutions needed by grid operations.

*Contributions.* This article makes the following contributions to the state-of-the-art in SC-ACOPF modeling and simulation. (i) We provide a systematic methodology for wildfire-aware SC-ACOPF that integrates geographic wildfire perimeter data with transmission network topology. This approach improves upon from the existing limited $N-1$ and $N-2$ contingencies by automatically generating realistic $N-k$ contingency scenarios that capture the spatially correlated nature of wildfire-driven outages. (ii) We formulate an integrated optimization problem that simultaneously optimizes base case operations and contingency responses, achieving real-time performance with solve times under three minutes for large-scale systems. (iii) We present illustrative numerical results for four recent major California wildfires. The results demonstrate both computational tractability and consistent economic benefits compared to sequential optimization, validating the practical value of integrated wildfire contingency planning for grid operations.

The remaining sections of this paper are organized as follows. We begin by providing in Section II an overview of the framework for the SC-ACOPF methodology for wildfire contingency planning. Next, in Section III we describe the problem setup, including the California test system and wildfire scenarios. Finally, in Section IV, we present the numerical experiments and economic analysis. Section V provides concluding remarks.

## II. Framework for integrating wildfires in SC-ACOPF-based power grid operations

This section presents an approach to construct wildfire-based contingency scenarios using historical fire perimeter data. The methodology uses geospatial analysis to identify grid components within defined threat zones around fire perimeters, automatically clustering at-risk equipment into realistic multi-component contingency scenarios. We first formulate the SC-ACOPF problem that incorporates these wildfire contingencies, then detail the spatial threat zone identification process.

### A. SC-ACOPF Model

We now formulate SC-ACOPF mathematically by defining the relevant variables. We will denote the set of buses by $\mathcal{N}$, the set of generators by $\mathcal{G}$, the set of branches by $\mathcal{E}$, and the set of credible contingencies by $\mathcal{K}$. The set of power flow cases will be denoted by $\mathcal{K}_0 = \mathcal{K} \cup \{0\}$, where 0 denotes the base case. For power flow case $k \in \mathcal{K}_0$ and generator $g \in \mathcal{G}$, let $p_{g,k}$ and $q_{g,k}$ be the active and reactive power, respectively. Additionally, at bus $n \in \mathcal{N}$, let $b_{n,k}$ be the variable shunt susceptance, and let $v_{n,k}$ and $\theta_{n,k}$ be the voltage magnitude and angle, respectively. Furthermore, to model constraint violations, let $\sigma_{e,o,k}$ and $\sigma_{e,d,k}$ be the overload of branch $e \in \mathcal{E}$ at its origin $o$ and destination $d$ buses, and $\sigma^P_{n,k}$ and $\sigma^Q_{n,k}$ be the active and reactive power imbalance, respectively. Finally $\delta_k$ is the frequency deviation in post-contingency case $k \in \mathcal{K}$.

The SC-ACOPF objective function consists of two components: the base-case cost $A(\boldsymbol{p}_0, \boldsymbol{\sigma}_0)$ and the average contingency cost $C(\boldsymbol{v}_k, \boldsymbol{\theta}_k, \boldsymbol{\sigma}_k)$. The base-case cost includes generation costs and penalties for any constraint violations and is given by

$$A(\boldsymbol{p}_0, \boldsymbol{\sigma}_0) = \sum_{g\in\mathcal{G}} C_g(p_{g,0}) + \sum_{e\in\mathcal{E}} (C_e(\sigma_{e,o,0}) + C_e(\sigma_{e,d,0})) + \sum_{n\in\mathcal{N}} \left(C^P_n(\sigma^P_{n,0}) + C^Q_n(\sigma^Q_{n,0})\right), \quad (1)$$

where $C_g(\cdot)$ is the piecewise linear cost function of generator $g \in \mathcal{G}$, $C_e(\cdot)$ is the piecewise linear convex penalization

function for overloading branch $e \in \mathcal{E}$, and $C_n^P(\cdot)$ and $C_n^Q(\cdot)$ are convex piecewise linear penalization functions for active and reactive power imbalance at bus $n \in \mathcal{N}$, respectively. The contingency cost averages penalties across all contingency scenarios reads

$$C(\boldsymbol{v}_k, \boldsymbol{\theta}_k, \boldsymbol{\sigma}_k) = \frac{1}{|\mathcal{K}|} \sum_{k \in \mathcal{K}} \Bigg( \sum_{e \in \mathcal{E}(k)} (\tilde{C}_e(\sigma_{e,o,k}) + \tilde{C}_e(\sigma_{e,d,k})) + \sum_{n \in \mathcal{N}} \big(\tilde{C}_n^P\big(\sigma_{n,k}^P\big) + \tilde{C}_n^Q\big(\sigma_{n,k}^Q\big)\big) + \gamma_v \sum_{n \in \mathcal{N}} v_{n,k}^2 + \gamma_\theta \sum_{n \in \mathcal{N}} \theta_{n,k}^2 \Bigg), \tag{2}$$

where $\tilde{C}_e(\cdot)$, $\tilde{C}_n^P(\cdot)$, and $\tilde{C}_n^Q(\cdot)$ are quadratic approximations of their base-case counterparts used in contingency scenarios for computational tractability [14], and $\gamma_v$ and $\gamma_\theta$ are penalty weights for voltage magnitude and angle deviations, respectively, that encourage solutions closer to nominal operating conditions.

The SC-ACOPF problem is subject to three types of constraint sets that ensure both technical feasibility and operational security. The first constraint enforces that the base-case operation satisfies all power flow equations, generator limits (active and reactive power bounds), variable shunt susceptance limits, branch thermal limits, voltage magnitude bounds, and power balance equations under normal operating conditions with all equipment in service. We define this by the base-case feasible set $\mathcal{D}(0)$. The second constraint ensures physically realistic transitions between the base case and post-contingency state $k$ by enforcing generator ramping constraints that limit the allowable change in active power output between scenarios while maintaining continuity of voltage variables and reactive power adjustments. We define this by the transition feasible set $\mathcal{T}(k)$. Finally, the third constraint guarantees that the system remains feasible under each contingency scenario by satisfying power flow equations and emergency operating limits with the affected components removed from service. These sets account for the same physical constraints as $\mathcal{D}(0)$ but apply emergency technical limits and consider only equipment that remains online after the contingency event. We define these by the post-contingency feasible sets $\mathcal{D}(k)$, $k \in \mathcal{K}$.

Using these cost functions and constraint sets, the SC-ACOPF problem is summarized as:

$$\min_{p,q,b,v,\theta,\delta,\sigma} \quad A(\boldsymbol{p}_0, \boldsymbol{\sigma}_0) + C(\boldsymbol{v}_k, \boldsymbol{\theta}_k, \boldsymbol{\sigma}_k) \tag{3}$$

subject to

$$(\boldsymbol{p}_0, \boldsymbol{q}_0, \boldsymbol{b}_0, \boldsymbol{v}_0, \boldsymbol{\theta}_0, \boldsymbol{\sigma}_0) \in \mathcal{D}(0) \tag{3a}$$

$$(\boldsymbol{p}_0, \boldsymbol{p_k}, \delta_k, \boldsymbol{v}_0, \boldsymbol{v}_k, \boldsymbol{q}_k) \in \mathcal{T}(k), \quad k \in \mathcal{K} \tag{3b}$$

$$(\boldsymbol{p}_k, \boldsymbol{q}_k, \boldsymbol{b}_k, \boldsymbol{v}_k, \boldsymbol{\theta}_k, \boldsymbol{\sigma}_k) \in \mathcal{D}(k), \quad k \in \mathcal{K}. \tag{3c}$$

This formulation provides the mathematical foundation for security-constrained optimal power flow under wildfire threats which will be described in subsection II-C.

### *B. Computational Solution Approach*

In this subsection, we describe the computational approach used to solve the SC-ACOPF problem formulated in (3). We note that this SC-ACOPF problem is a large-scale nonlinear nonconvex optimization problem that becomes computationally demanding as the number of contingencies grows. Traditional $N-1$ contingency already presents significant computational challenges for realistic power systems; incorporating wildfire-driven $N-k$ contingencies—where multiple components fail simultaneously—further increases problem size and complexity. Each additional contingency scenario introduces thousands of additional variables and constraints corresponding to the post-contingency power flow equations and operating limits.

To solve the wildfire-driven $N-k$ contingency SC-ACOPF problem, we extend the state-of-the-art solver ExaJuGO [21] to support multi-element contingency scenarios induced by wildfire forecasts. ExaJuGO is a high-performance optimization solver specifically designed for large-scale power grid applications. It is developed in Julia for efficient numerical computation and employs the interior-point optimizer Ipopt [22], which is particularly well-suited for the nonlinear and inequality-constrained nature of the SC-ACOPF problem. For the critical linear algebra operations within each interior-point iteration, ExaJuGO utilizes the MA57 sparse direct solver [11] to efficiently handle the large, sparse, symmetric indefinite systems that arise from the problem's Karush-Kuhn-Tucker (KKT) optimality conditions [13].

The extension we added to ExaJuGO (to support wildfire contingencies) required modifications to handle arbitrary $N-k$ outage patterns where the set of offline components varies across scenarios, as opposed to traditional $N-1$ where contingencies follow predictable single-component patterns. This capability now enables ExaJuGO to process the spatially correlated multi-component outages characteristic of wildfire events, as described in the following subsection.

### *C. Wildfire Contingency Modeling*

Having established the SC-ACOPF formulation and computational solution approach, we now detail the methodology for systematically generating the wildfire-driven contingency scenarios that populate the set $\mathcal{K}$ in (3). Unlike traditional $N-1$ or $N-2$ contingencies that assume independent component failures, wildfire contingencies involve spatially correlated, simultaneous outages of multiple transmission lines, transformers, and generators determined by the geographic spread of fire events. This subsection presents how historical wildfire perimeter data is integrated with transmission network topology to identify at-risk components and how to construct realistic multi-component contingency scenarios for the SC-ACOPF problem.

The methodology centers on defining threat zones using a critical parameter termed the "safe distance" (SD), which establishes the minimum allowable separation between fire perimeters and grid infrastructure. This threshold incorporates

radiant heat effects, ember transport distances, and operational safety margins based on established wildfire evacuation protocols. Components located beyond the SD threshold are considered secure and remain in service, while those within this buffer zone are classified as exposed and must be removed from service in the contingency. Figure 1 illustrates this approach for the January 2025 Eaton fire in Los Angeles County, where the grey area represents the fire perimeter and the orange buffer zone defines the threat area. Transmission lines and generators within this threat zone (shown in red) are identified as at-risk components that must be simultaneously removed to form the wildfire contingency scenario.

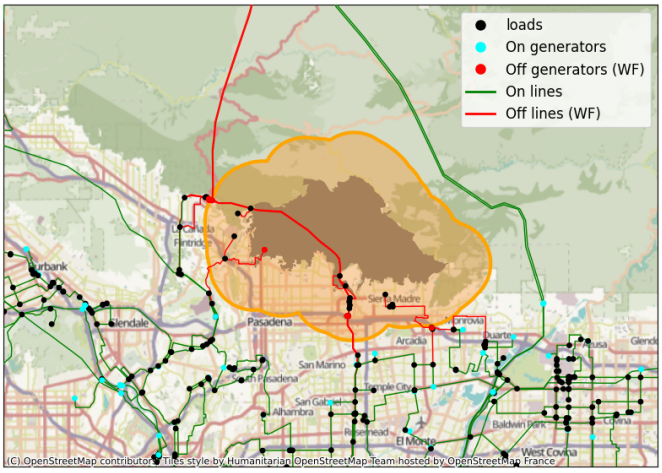


Fig. 1. Wildfire threat zone identification for the January 2025 Eaton fire (grey area) with threat zone (orange area) at safe distance SD. At-risk components within the buffer (red lines and dots) are removed to create the contingency scenario, while secure components outside the buffer (green lines and cyan dots) remain in service.

The integration process operates as follows: (1) wildfire perimeter data are obtained from historical records or real-time fire monitoring systems, (2) a threat zone of radius SD is constructed around each fire perimeter using geospatial analysis, (3) transmission network component locations are compared against the buffer zones to identify at-risk equipment, and (4) all identified at-risk components are grouped to form a single wildfire contingency scenario that represents the simultaneous forced outage event. This approach systematically generates contingency scenarios that capture the spatially correlated nature of wildfire threats, which traditional contingency methods cannot represent.

The methodology's accuracy depends critically on appropriate calibration of the parameter SD, which should reflect local fire behavior characteristics, vegetation density, terrain features, wind patterns, and grid design standards. This framework provides power system operators with essential tools for proactive wildfire risk management and enables evaluation of system resilience under increasingly frequent climate-driven threats.

## III. Problem Setup

This section demonstrates the practical application of the wildfire contingency methodology presented in Section II-C through a comprehensive analysis of California's transmission grid under historical wildfire scenarios. We first introduce the California Test System (CATS) [17], a geographically accurate synthetic grid model that enables realistic wildfire impact assessment. We then describe the historical wildfire data sources used to generate the contingency scenarios that populate the set $\mathcal{K}$ in the SC-ACOPF formulation (3). The combination of geographically accurate grid data and real wildfire perimeters enables quantification of both the physical grid impacts and operational costs under wildfire threats.

### A. The California Test System (CATS)

To effectively study wildfire impacts on power systems, we require a test system that accurately represents both the electrical characteristics and geographic layout of the transmission network. The CATS model represents a significant advancement in power systems research by providing the first publicly available synthetic transmission grid model that maintains a geographically accurate representation of California's electrical infrastructure. This synthetic grid combines publicly available geographic data of California's actual transmission corridors with realistic but synthetic topology and transmission line parameters, creating a model suitable for research without compromising critical energy infrastructure information.

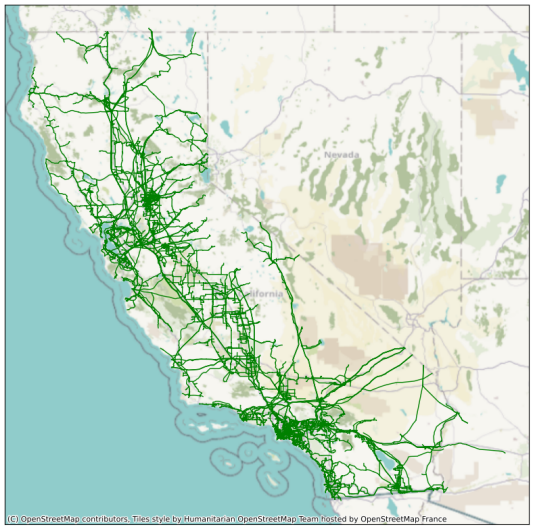


Fig. 2. CATS grid overlaid on the California map.

The CATS model encompasses 8,870 buses with 10,162 transmission lines and 661 transformers, serving 2,472 load buses with a peak load of 44,009 MW. The system includes 2,149 generators with a total capacity of 73,172 MW. Unlike traditional IEEE test cases that lack geographic information, CATS provides accurate transmission line paths that follow real topography, vegetation, and property boundaries rather

than simple point-to-point connections. This geographic fidelity is essential for wildfire contingency, as it enables accurate identification of grid components within fire threat zones based on their actual spatial locations. Figure 2 illustrates the CATS network overlaid on the California map, showing the extensive coverage of transmission infrastructure across diverse geographic regions exposed to varying wildfire risks.

### B. Wildfire Data Sources

Historical wildfire perimeter data are obtained from the National Interagency Fire Center (NIFC) [12], which provides observed fire extents captured during active fire events. These perimeters represent the geographic footprint of wildfires at specific points in time, typically before full containment. For this study, we focus on four significant California wildfires: the Bridge, Fawn, and Monument fires from 2021, and the more recent Eaton fire from 2025. These fires were selected based on their proximity to major transmission corridors and their varying geographic locations across California, providing diverse test cases for evaluating our methodology's effectiveness across different grid regions and fire characteristics.

We evaluate our methodology across these four wildfires using three safe distance (SD) values: 2, 6, and 12 miles. These distances align with the California utility operational protocols, which use approximately $1.5 \times 1.5$ mile grid cells for PSPS decisions, with threat radii ranging from 500 feet (firefighting zones) to many miles (extreme wind events) based on Fire Potential Index modeling [10]. Hence, the proposed values span conservative (SD = 2), moderate (SD = 6), and extreme (SD = 12 miles) scenarios. Table I summarizes the resulting contingency scenarios, showing the number of transmission lines, transformers, and generators identified as at-risk within each buffer zone, as well as the network fragmentation (number of islands created) when these components are removed.

TABLE I
WILDFIRE CONTINGENCY SCENARIOS: AFFECTED COMPONENTS AND NETWORK FRAGMENTATION

| Wildfire | SD (miles) | Off Lines | Off Trans. | Off Gens. | Islands Created |
|---|---|---|---|---|---|
| Bridge | 2 | 6 | 0 | 1 | 0 |
| | 6 | 21 | 1 | 7 | 0 |
| | 12 | 32 | 1 | 10 | 1 |
| Fawn | 2 | 11 | 1 | 0 | 1 |
| | 6 | 47 | 6 | 3 | 1 |
| | 12 | **99** | **9** | 10 | **3** |
| Monument | 2 | 4 | 0 | 0 | 0 |
| | 6 | 16 | 3 | 0 | 1 |
| | 12 | 25 | 4 | 1 | 1 |
| Eaton | 2 | 46 | 3 | 8 | 0 |
| | 6 | 178 | 6 | 30 | 0 |
| | 12 | **591** | **18** | **99** | 1 |

This table reveals substantial variation in contingency severity across fires and safe distances. The Monument fire affects relatively few components even at SD 12 (25 lines, 4 transformers, 1 generator), while the Eaton fire creates the most severe scenarios, with 591 lines, 18 transformers, and 99 generators removed at SD 12. Network fragmentation also varies significantly: some scenarios maintain network connectivity (no islands created), while others fragment the grid into multiple disconnected subnetworks—most notably the Fawn fire at SD 12, which creates 3 additional islands beyond the main network. We note that, when an AC network contains islands, the underlying Jacobian matrix drops in rank, which causes the single-reference bus model to fail [23]. To avoid this computational challenge, the solver we propose dynamically assigns a new reference bus for each island. This modification allows us to include extreme grid and wildfire characteristics which enables a comprehensive evaluation of the SC-ACOPF methodology at various levels of grid stress.

## IV. Numerical Experiments

This section presents the computational results and economic analysis of the SC-ACOPF methodology applied to the twelve wildfire scenarios defined in Section III. We first report on the solver performance and computational requirements for solving these large-scale security-constrained optimization problems. We then evaluate the economic benefits of the integrated SC-ACOPF formulation by comparing it against a sequential optimization approach, examining both the physical grid impacts and the cost savings achieved through simultaneous base case and contingency optimization.

### A. Solver Performance

Table II presents the computational performance metrics for all twelve wildfire scenarios. The SC-ACOPF formulation results in a large-scale nonlinear optimization problem with 255,761 variables and approximately 225,000 constraints (specific counts vary by scenario due to different numbers of affected components). The solver was configured with a convergence tolerance of $10^{-6}$ for optimality and constraint violations, with acceptable solution criteria of 0.01 for dual infeasibility, $10^{-6}$ for constraint violations, and 0.01 for complementarity.

As shown by the color gradient in Table II, solve times ranged from 59.0 to 140.5 seconds with an average of 102.7 seconds, with all scenarios solving in under three minutes. The results demonstrate that the methodology achieves real-time computational performance suitable for operational decision-making as wildfire conditions evolve. We note that the computational requirements did not scale strictly with the number of affected components or network islands created—the most severe scenario (Eaton SD 12: 591 lines, 18 transformers, 99 generators, 1 island) required 132.0 seconds while the smallest scenario (Monument SD 2: 4 lines, 0 islands) required 140.5 seconds. Similarly, the Fawn SD 12 scenario with 3 islands was solved in just 83.6 seconds. These results suggest that problem structure and network topology influence computational complexity beyond simple component counts or network fragmentation. Iteration counts ranged from 73 to

TABLE II
REAL-TIME SOLVER PERFORMANCE FOR WILDFIRE SC-ACOPF SCENARIOS (ALL SCENARIOS SOLVE IN UNDER 3 MINUTES).

| Wildfire | SD (miles) | Iterations | Solve Time (s) |
|---|---|---|---|
| Bridge | 2 | 157 | 111.5 |
| | 6 | 168 | 126.0 |
| | 12 | 159 | 113.2 |
| Fawn | 2 | 145 | 105.6 |
| | 6 | 103 | 80.7 |
| | 12 | 104 | 83.6 |
| Monument | 2 | 184 | **140.5** |
| | 6 | 156 | 121.7 |
| | 12 | 103 | 86.0 |
| Eaton | 2 | 87 | 72.4 |
| | 6 | 73 | **59.0** |
| | 12 | 154 | 132.0 |

184, demonstrating that ExaJuGO efficiently handles the large-scale nonconvex optimization problems arising from wildfire contingencies.

### B. Operational Performance

We now evaluate the economic value of the SC-ACOPF formulation by comparing it against a sequential optimization approach. The key question is whether simultaneously optimizing base case operations and wildfire contingencies provides measurable benefits compared to solving these problems independently.

In the sequential approach, the base case problem minimizes (1) subject to (3a), determining generation dispatch without considering contingencies. Subsequently, each contingency subproblem minimizes (2) subject to (3b) and (3c), given the fixed base case decisions. The total cost from this sequential approach—which we call the "realized cost"—is the sum of these independently solved problems. In contrast, our SC-ACOPF approach optimizes the base case and all contingencies simultaneously through the formulation (3)–(3c), achieving lower total costs through coordination. The economic benefit of our approach is measured by:

$$\text{Benefit} = \frac{\text{Realized Cost} - \text{SC-ACOPF Objective}}{\text{Realized Cost}} \times 100\%,$$

where positive values indicate cost savings from simultaneous optimization.

*1) Physical Grid Impacts:* Figure 3 illustrates the cascading effects of the Monument wildfire with a 12-mile safe distance on California's power grid. This visualization reveals that the grid's response extends far beyond the fire perimeter—power flows redistribute across the entire California network. Lines colored in yellow and red indicate increased loading as the system reroutes electricity around compromised infrastructure within the threat zone, while blue regions show decreased flows due to lost generation or transmission capacity. This statewide redistribution demonstrates how localized wildfire

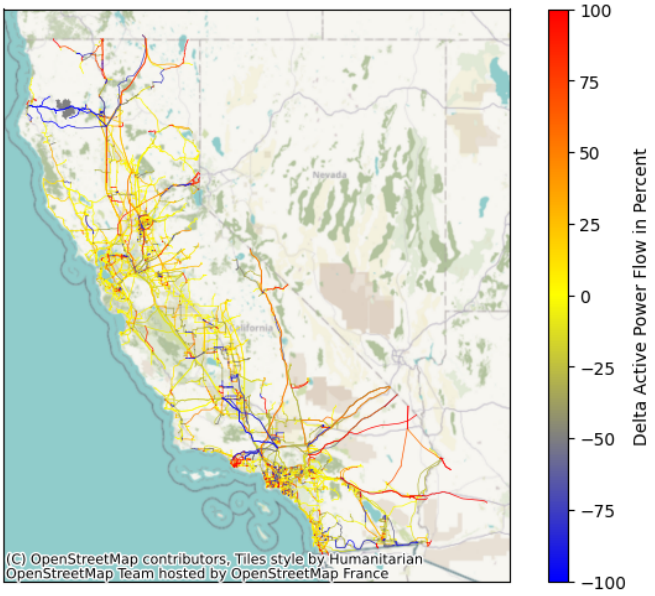


Fig. 3. Statewide power flow changes (as percentage of line capacity) for Monument wildfire with 12-mile safe distance showing redistribution patterns across California's transmission network.

events trigger system-wide operational adjustments, underscoring the interconnected nature of transmission networks and the need for comprehensive contingency planning.

*2) Economic Performance:* Table III compares the SC-ACOPF objective values against realized costs for all twelve test scenarios. The results reveal that the integrated SC-

TABLE III
ECONOMIC COMPARISON OF INTEGRATED SC-ACOPF VERSUS SEQUENTIAL OPTIMIZATION.

| Wildfire | SD (miles) | SC-ACOPF Objective ($) | Realized Cost ($) | Benefit (%) |
|---|---|---|---|---|
| Bridge | 2 | 878K | 881K | 0.28% |
| | 6 | 1,278K | 1,286K | 0.66% |
| | 12 | 1,371K | 1,400K | 2.14% |
| Fawn | 2 | 794K | 797K | 0.30% |
| | 6 | 839K | 841K | 0.29% |
| | 12 | 995K | 1,136K | **14.19%** |
| Monument | 2 | 793K | 796K | 0.32% |
| | 6 | 873K | 876K | 0.33% |
| | 12 | 962K | 965K | 0.31% |
| Eaton | 2 | 1,977K | 1,980K | 0.15% |
| | 6 | 14,516K | 14,518K | 0.02% |
| | 12 | 113,256K | 113,493K | 0.21% |

ACOPF approach achieves lower costs than sequential optimization across all twelve scenarios, with benefits ranging from 0.02% to 14.19%. Several additional specific conclusions can be drawn from this table. First, larger safe distances generally yield greater economic benefits, particularly for the Bridge and Fawn fires where savings increase substantially from SD 2 to SD 12. This suggests that coordination becomes more valuable when more infrastructure must be simultaneously

removed from service—consistent with the component counts shown in Table I. Second, fire-specific factors significantly influence optimization benefits: the Fawn fire at SD 12 achieves the largest improvement (14.19%), while the Monument fire shows consistent but modest benefits ($\approx 0.3\%$) regardless of safe distance. Third, the Eaton fire presents an interesting case where despite affecting substantially more infrastructure (591 lines, 18 transformers, and 99 generators at SD 12), relative benefits remain modest (0.02-0.21%), likely due to the fire's location in a highly constrained urban region with limited operational flexibility.

Finally, we note that even small percentage improvements translate to meaningful absolute savings—for example, the 0.02% benefit for Eaton SD 6 represents approximately $2,900 in operational cost reduction. These results confirm that integrated optimization provides tangible economic value across diverse wildfire scenarios, with particularly significant benefits when contingencies affect large portions of the transmission network. The methodology's effectiveness varies by fire location and grid topology, but consistently demonstrates the advantage of simultaneous base case and contingency optimization over sequential approaches.

## V. Conclusion

This work develops a systematic methodology for wildfire-aware security-constrained AC optimal power flow that captures the spatially correlated, simultaneous outages characteristic of wildfire events. By integrating historical wildfire perimeter data with transmission network topology through configurable safe distance parameters, the approach automatically generates realistic $N-k$ contingency scenarios—a significant departure from traditional $N-1$ or $N-2$ contingencies that assumes independent component failures.

The methodology achieves real-time computational performance across twelve test scenarios, with solve times ranging from 59 to 141 seconds for problems containing 255,761 variables and approximately 225,000 constraints. Notably, computational requirements did not correlate with problem severity, as scenarios with hundreds of affected components were solved in comparable times to minimal-impact scenarios, indicating that network topology dominates computational complexity over component counts. Economic analysis across four California wildfires revealed consistent benefits ranging from 0.02% to 14.19% compared to sequential optimization, with the most severe scenario achieving $141K in savings. The methodology's transferability to other weather-driven threats provides power system operators with practical tools for climate-resilient grid operations.

## Acknowledgments

This work was performed under the auspices of the U.S. Department of Energy by Lawrence Livermore National Laboratory under contract DE–AC52–07NA27344. Release number LLNL-PROC-2015938 and supported at LLNL by the U.S. Department of Energy through the Scientific Discovery through Advanced Computing (SciDAC) program under the ASCR–OE SLOPE-Grid partnership. N. P. and R. M acknowledge NSF DMS Grant 2229495 and UCOP Climate Action Seed Funds.

## References

[1] I. Aravena, D. K. Molzahn, S. Zhang, C. G. Petra, F. E. Curtis, S. Tu, A. Wächter, E. Wei, E. Wong, A. Gholami, *et al.*, "Recent developments in security-constrained AC optimal power flow: Overview of challenge 1 in the ARPA-E grid optimization competition," *Operations Research*, vol. 71, no. 6, pp. 1997–2014, 2023.

[2] R. S. Biswas, A. Pal, T. Werho, and V. Vittal, "Mitigation of saturated cut-sets during multiple outages to enhance power system security," *IEEE Transactions on Power Systems*, 36 (6), pp. 5734–5745, 2021.

[3] J. Carpentier, "Optimal power flows," *International Journal of Electrical Power & Energy Systems*, vol. 1, no. 1, pp. 3–15, 1979.

[4] A. Castillo and R. P. O'Neill, *Survey of Approaches to Solving the ACOPF (OPF Paper 4)*. Washington, DC, USA: Federal Energy Regulatory Commission, Tech. Rep., 2013. [Online]. Available: https://www.ferc.gov/sites/default/files/2020-05/acopf-4-solution-techniques-survey.pdf

[5] P. L. Donti, A. Agarwal, N. V. Bedmutha, L. Pileggi, and J. Z. Kolter, "Adversarially robust learning for security-constrained optimal power flow," in *Advances in Neural Information Processing Systems (NeurIPS)*, vol. 34, 2021. [Online]. Available: https://proceedings.neurips.cc

[6] Elmfire Project, *Getting Started with Elmfire*, 2025. [Online]. Available: https://elmfire.io/index.html

[7] Grid Optimization Competition, *SCOPF Problem Formulation: Challenge 1*, 2019. [Online]. Available: https://gocompetition.energy.gov/challenges/challenge-1/formulation

[8] R. Harris, C.-Y. Chang, and D. K. Molzahn, "Integrated transmission-distribution multi-period switching for wildfire risk mitigation: Improving speed and scalability with distributed optimization," in *Proc. IEEE Kiel PowerTech*, June 2025.

[9] M. Ilić, L. L. Anton, and R. Jaddivada, "AC-extended optimal power flow (AC XOPF) for reliable grid operations and planning in support of energy transition: Puerto Rico power grid case," in *IET Conference Proceedings*, vol. 2024, no. 29, pp. 142–149, 2024, doi: 10.1049/icp.2024.4651.

[10] Pacific Gas and Electric Company, "Public Safety Power Shutoff Post-Event Report: January 22, 2025," PG&E Technical Reports, 2025.

[11] I. S. Duff, "MA57—a code for the solution of sparse symmetric definite and indefinite systems," *ACM Transactions on Mathematical Software (TOMS)*, vol. 30, no. 2, pp. 118–144, 2004.

[12] National Interagency Fire Center, *Wildland Fire Summary and Statistics Annual Report*, 2023. [Online]. Available: https://www.nifc.gov/fire-information/statistics

[13] J. Nocedal and S. J. Wright, *Numerical Optimization*. Springer, 2006.

[14] C. G. Petra and I. Aravena, "A surrogate-based asynchronous decomposition technique for realistic security-constrained optimal power flow problems," *Operations Research*, vol. 71, no. 6, pp. 2015–2030, 2023.

[15] N. Rhodes and L. A. Roald, "Co-optimization of power line shutoff and restoration under high wildfire ignition risk," in *Proc. IEEE Belgrade PowerTech*, 2023, pp. 1–7.

[16] S. Sahoo and A. Pal, "Cut-set and stability constrained optimal power flow for resilient operation during wildfires," in *Proc. IEEE Kansas Power and Energy Conference (KPEC)*, 2024, pp. 1–6.

[17] S. Taylor, A. Rangarajan, N. Rhodes, J. Snodgrass, B. C. Lesieutre, and L. A. Roald, "California test system (CATS): A geographically accurate test system based on the California grid," *IEEE Transactions on Energy Markets, Policy and Regulation*, vol. 2, no. 1, pp. 107–118, 2024, doi: 10.1109/TEMPR.2023.3338568.

[18] A. Venzke, S. Chatzivasileiadis, and D. K. Molzahn, "Inexact convex relaxations for AC optimal power flow: Towards AC feasibility," *Electric Power Systems Research*, vol. 187, p. 106480, 2020.

[19] H. Yang, N. Rhodes, H. Yang, L. A. Roald, and L. Ntaimo, "Multi-period power system risk minimization under wildfire disruptions," *IEEE Transactions on Power Systems*, vol. 39, no. 5, pp. 6305–6318, 2024.

[20] R. Yao, F. Qiu, and K. Sun, "Contingency analysis based on partitioned and parallel holomorphic embedding," *IEEE Transactions on Power Systems*, vol. 37, no. 1, pp. 565–575, 2021.

[21] Lawrence Livermore National Laboratory, *ExaJuGO: Extreme-scale Nonlinear Programming*, 2024. [Online]. Available: https://github.com/LLNL/exajugo

[22] COIN-OR Foundation, *Ipopt: Interior Point Optimizer*, 2025. [Online]. Available: https://github.com/coin-or/Ipopt
[23] B. Stott and O. Alsac, "Fast decoupled load flow," *IEEE Transactions on Power Apparatus and Systems*, vol. 93, no. 3, pp. 859–869, 1974.